CHEMISTRY
A EUROPEAN JOURNAL

DOI: 10.1002/chem.201100559

Towards Larger Polygonal Architectures: Synthesis and Characterization of Iron(II)– and Ruthenium(II)–Bis(terpyridine) Metallomacrocycles

Yi-Tsu Chan, Xiaopeng Li, Charles N. Moorefield, Chrys Wesdemiotis,* and George R. Newkome*[a]

Construction of supramolecular architectures employing the self-assembly of predesigned building blocks has drawn considerable attention in the past decades.[1] Based on the combinatorial library proposed by Lehn,[2] self-assembling constructs are often an equilibrium distribution of possible assemblies possessing comparable stabilities. Assemblies with similar components resulting in an equilibrating mixture of binary[2a,c,3] or multiple[4] entities have been reported. Under appropriate conditions, the thermodynamically most stable species can be obtained in quantitative yield. Based on these tenants, many successful strategies have been developed for the synthesis of metallocycles with triangular,[5] rectangular,[6] pentagonal,[7] and hexagonal[8] shapes. In contrast, few examples of larger polygonal structures are documented.[9] Towards larger finite architectures, subtle variation of building blocks could result in a dramatic change to the final products.[10] In the self-assembly of bis(terpyridine) ligands possessing a 120° angle between two ligating moieties, only hexameric metallomacrocycles were previously reported due to the difficulty of separation and characterization.[8b–d] More recently, Newkome et al. successfully isolated unexpected pentameric[7a] and heptameric[11] macrocycles from the Fe^{II}-mediated complexation of rigid bis(terpyridine) ligands. Herein, we employ kinetically stable <tpy-M^{II}-tpy> (in which tpy = 2,2′:6′,2″-terpyridine, M = Fe and Ru)[12] connectivity to afford a series of homo- and heteronuclear metallomacrocycles by means of stepwise assembly procedures. By using metals that form strong coordinative bonds (Fe^{II} and Ru^{II}), the self-assembly process becomes kinetically controlled and irreversible, thus allowing for the formation of macrocycles other than the thermodynamically most stable hexameric ring.[12c] Further, the use of elongated bis(terpyridine) dimers as precursors introduces steric constraints and increased rotational freedom, which obstruct the formation of small metallocycles, while facilitating the construction of novel, large metallocycles that would be difficult to realize otherwise. Traveling-wave ion-mobility mass spectrometry (TWIM-MS)[8g,11,13] and molecular modeling provide unique insight into the distinct ring sizes formed and their conformational flexibility.

Reaction (Scheme 1a) of 3,5-bis(4′-terpyridinyl)anisole (**1**) with 1.05 equivalents of $FeCl_2{\cdot}4H_2O$ in a mixed solvent of MeOH/$CHCl_3$ at reflux for 18 h gave the pentamer (**2**; 6%), hexamer (**3**; 15%), and heptamer (**4**; 3%), which were isolated by column chromatography (SiO_2) eluting with H_2O/MeCN/sat.-KNO_3(aq) (1:12.5:1; v/v/v). Subsequently, the counterions were exchanged from NO_3^- to PF_6^- by adding a slight excess of methanolic NH_4PF_6 (1 M). The ^{1}H NMR spectrum (Figure S1a in the Supporting Information) of pentamer **2** displayed four sharp singlets at $\delta = 9.41$ (3′,5′-tpy*H*), 8.61 (4-Ar*H*), 8.16 (2,6-Ar*H*) and 4.34 ppm (OCH_3), supporting the presence of a single homogeneous environment for complexed bis(terpyridine) ligands, in contrast to linear oligomers that have more complicated patterns.[14] Other supportive data included an expected upfield shift in the ^{1}H NMR spectrum for the 6,6″-tpy*H* protons ($\delta = 7.27$ ppm, $\Delta\delta = -1.48$ ppm) relative to the corresponding peaks of ligand **1** and one sharp peak in the ^{13}C NMR spectrum at $\delta = 57.3$ ppm (OCH_3). Its structure was further confirmed by the intense ESI-MS peaks (Figure S2a in the Supporting Information) at *m*/*z* 1382.7, 1000.4, 771.3, 618.6, 509.5, and 427.7, corresponding to $[M-n\,PF_6]^{n+}$ ions ($n = 3$–8), respectively. The ^{1}H NMR spectra of macrocycles **3** and **4** revealed similar patterns, but all aromatic peaks exhibited a slight downfield shift relative to the corresponding peaks in **2**, presumably due to conformational changes in the larger rings. The 4-Ar*H* signal in pentamer **2** showed a significant upfield shift ($\Delta\delta = -0.13$ ppm) in comparison with hexamer **3**, owing to the shielding by the adjacent pyridines in the more crowded inner space (Figure S1b in the Supporting Information). A similar phenomenon was observed in our previous work.[7a] Heptamer **4** has more conformational flexibility, minimizing this shielding effect; its 4-Ar*H* signal was shifted further downfield (Figure S1c in the Supporting Information). Macrocycles **3** (MW = 5498.5 Da) and **4** (MW = 6414.9 Da) were further verified by their ESI mass spectra (Figure S2b and S2c in the Supporting Information). Hexamer **3** gave rise to eight major peaks at *m*/*z* 1229.7, 954.7,

[a] Dr. Y.-T. Chan,[+] Dr. X. Li,[+] Dr. C. N. Moorefield, Prof. Dr. C. Wesdemiotis, Prof. Dr. G. R. Newkome
Department of Polymer Science, Department of Chemistry
The University of Akron, 170 University Circle-RM501B
Akron, OH 44325-4717 (USA)
Fax: (+1) 330-972-2368
E-mail: newkome@uakron.edu
wesdemiotis@uakron.edu
Homepage: http://www.dendrimers.com

[+] Drs. Chan and Li contributed equally to this work.

Supporting information for this article is available on the WWW under http://dx.doi.org/10.1002/chem.201100559.

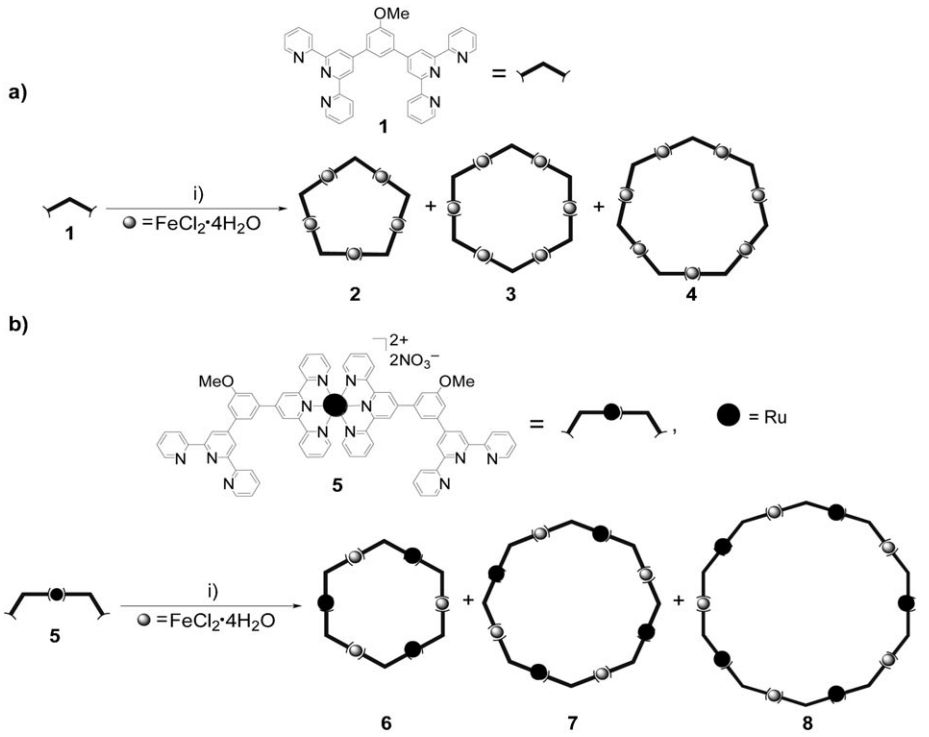

Scheme 1. a) Fe^{II} macrocycles **2**–**4** obtained by the macrocyclization of **1**. b) Ru^{II}–Fe^{II} macrocycles **6**–**8** was similarly obtained from **5**. Reaction conditions: i) $FeCl_2{\cdot}4H_2O$, MeOH, reflux, 18 h. (each macrocycle isolated as the polyPF_6^- salt).

771.4, 640.5, 542.3, 465.9, 404.9, and 354.8, which correspond to species with +4 to +11 charges, respectively; whereas, heptamer **4** displayed nine intense peaks at *m*/*z* 1459.0, 1138.0, 924.1, 771.4, 656.8, 567.7, 496.5, 438.2, and 389.6, which agree with multiply-charged entities having +4 to +12 charges.

From a single-pot reaction of bis(terpyridine) ligand **1** with 0.5 equivalents of $[RuCl_2(dmso)_4]$, the $[Ru(\mathbf{1})_2(NO_3)_2]$ dimer **5** was isolated in 29% yield after employing column chromatography (basic Al_2O_3; eluent: H_2O/MeCN/sat.-KNO_3(aq), 1:30:1 v/v/v). Reaction (Scheme 1b) of the $[Ru(\mathbf{1})_2(NO_3)_2]$ dimer **5** with 1.05 equivalents of $FeCl_2{\cdot}4H_2O$ in MeOH afforded hexamer (**6**; 36%), octamer (**7**; 9%), and decamer (**8**; 2%), which were also isolated by column chromatography (SiO_2; eluent: H_2O/MeCN/sat.KNO_3(aq), 1:10:1 v/v/v). The alternating Ru^{II}–Fe^{II} sequence in the macrocycles resulted in more complicated ^{1}H NMR patterns (Figure 1), exhibiting two sets (Ru^{II} and Fe^{II} complexes) of signals for the terpyridine units. The ^{1}H NMR spectrum of heteronuclear hexamer **6** exhibited four sharp singlets at $\delta =$ 9.42 (Fe^{II}; 3′,5′-tpy*H*), 9.28 (Ru^{II}; 3′,5′-tpy*H*), 8.64 (4-Ar*H*), and 4.31 ppm (OCH_3), supporting the symmetric macrocyclic architectures. Other proof included a diagnostic upfield shift for the 6,6″-tpy*H* proton signals ($\delta = 7.29$ ppm, $\Delta\delta = -1.47$ ppm) of Fe^{II} complexes and two sharp singlets at $\delta =$ 8.14 and 8.08 ppm assigned to the 2,6-Ar*H* protons resulting from the neighboring Ru^{II} and Fe^{II} coordination. The hexagonal motif was further verified by the ESI-MS signals (Figure 2a) for the multiply-charged species in charge states 4+ to 9+. The ^{1}H NMR spectra of heteronuclear metallomacrocycles **7** and **8** showed similar patterns to that of **6**, but a significant downfield shift ($\delta =$ 8.71 ppm, $\Delta\delta = +0.07$ ppm) for the inner 4-Ar*H* protons relative to the corresponding peak of **6** (Figures 1b and c). Lastly, the structures of octamer **7** and decamer **8** were established by their distinctive ESI-MS spectra (Figure 2b and c).

TWIM-MS and molecular modeling were applied to validate the structures of these different macrocycles. The ESI and ion-mobility process were optimized (see Supporting Information) to reduce fragmentation. Different charge states of each macrocycle were separated by ion mobility (Figure 3 and Figures S3–S7 in the Supporting Information), after which mainly intact macrocycles are observed. For this, the

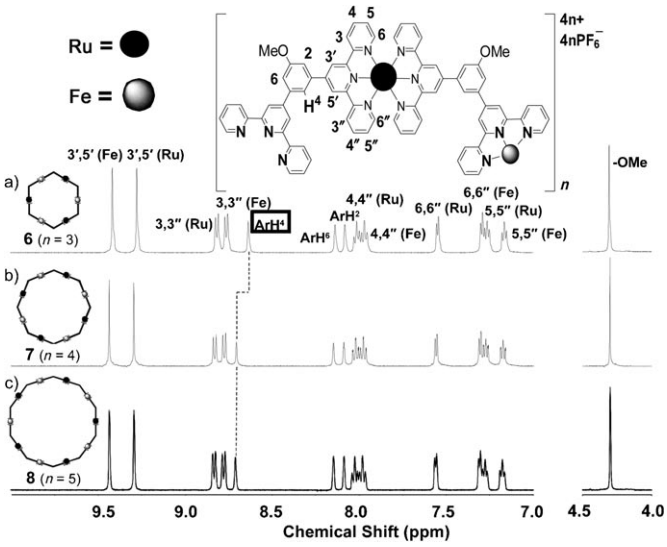

Figure 1. ^{1}H NMR spectra of a) hexamer **6**, b) octamer **7**, and c) decamer **8**.

potentials across the ESI source and ion entrance into the vacuum system must be kept low (see Supporting Information). Elevated potentials can cause fragmentation and ring-opening.[8g,11,13a,b,15] In the present study, different cyclic conformers, instead of cyclic and ring-opened isomers,[8g,11,13a,b,15] were observed for ions in specific charge states. For instance, the 5+ ions of heptamer **4** contained two structures, drifting

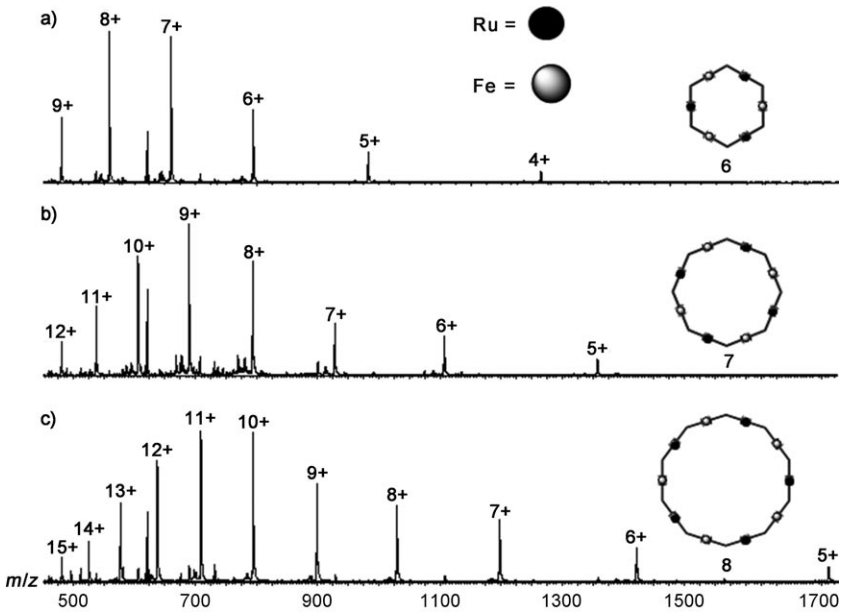

Figure 2. ESI-MS spectra of a) hexamer **6**, b) octamer **7**, and c) decamer **8**.

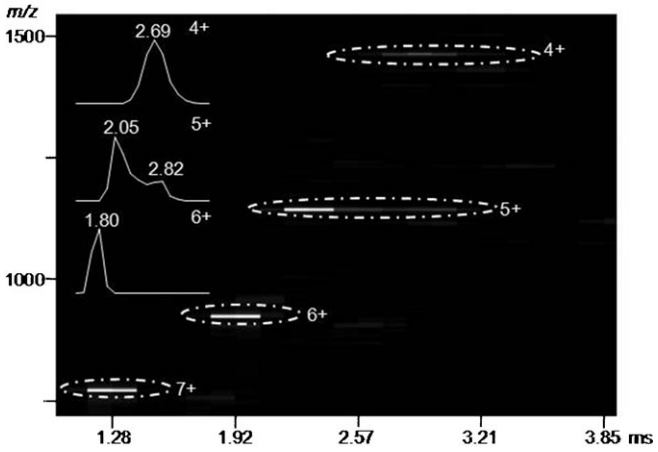

Figure 3. Two-dimensional ESI-TWIM-MS plot of heptamer **4**, covering charge states 4+ to 7+ and acquired at a traveling wave velocity of 350 m s^{-1} and a traveling-wave height of 11 V. The insets show the drift time distributions of 4+, 5+, and 6+ ions; the distribution of the 7+ ions is similar to those observed for the 4+ and 6+ charge states (unimodal).

out at 2.05 and 2.82 ms; whereas, only a single structure was observed for the ions with 4+, 6+, and 7+ charges (Figure 3). If ring-opened isomers existed, distinct drift time distributions for cyclic and linear species should have been observed at all charge states, with the corresponding peaks becoming increasingly resolved with the number of charges;[8g,11] however, only ions at a few specific charge states exhibited multiple peaks after ion-mobility separation. Thus, it was concluded that cyclic conformers were being separated at these charge states. Two different conformers were observed for 5+ ions from heptamer **4**, as noted above, as well as for 4+ ions from hexamers **3** and **6**; whereas, three conformers were detected for 5+ ions from octamer **7**. In contrast, multiple conformers were observed for the 5+, 6+, 7+, and 8+ ions derived from decamer **8**. For the smallest macrocycle, namely, **2**, only one conformer was observed due to the low flexibility of this ring size.

Experimental collision cross-sections were obtained by calibrating the drift timescale[16] of our TWIM device (Figure S8 in the Supporting Information) and are summarized in Table 1. For the collision cross-sections of the smallest macrocycle, namely, the pentamer, no significant charge dependence was found. A similar observation was recently reported by Bowers et al. for small rigid triangular and rectangular struc-

Table 1. Experimental and calculated collision cross-sections (CCS) of metallocycles.

	Exptl CCS [Å^2][a]	Average exptl CCS [Å^2]	Calcd CCS (STDEV) [Å^2][b]
2	692.3 (3+)	685.9	640.0 (4.8)
	679.4 (4+)		
3	698.7 (3+)	771.6	767.5 (6.8)
	725.9 (4+)		
	848.4 (4+)		
	813.4 (5+)		
4	782.4 (4+)	887.7	901.0 (10.6)
	846.3 (5+)		
	991.1 (5+)		
	930.9 (6+)		
6	701.6 (3+)	795.6	773.7 (6.0)
	821.5 (4+)		
	852.5 (4+)		
	806.9 (5+)		
7	695.2 (5+)	914.1	1028.2 (13.2)
	873.2 (5+)		
	997.1 (5+)		
	964.9 (6+)		
	1040.2 (7+)		
8	837.7 (5+)	1179.2	1195.0 (114.5)
	1055.8 (5+)		
	1162.9 (5+)		
	993.7 (6+)		
	1199.3 (6+)		
	1131.6 (7+)		
	1457.6 (7+)		
	1236.8 (8+)		
	1407.3 (8+)		
	1309.8 (9+)		

[a] Collision cross-section (CCS) obtained by calibrating the drift time scale of the TWIM device with standards of known cross-sectional data (calibration plot shown in Figure S8). [b] Obtained from the energy-minimized structures deduced computationally using the DriftScope 2.1 software with the projection approximation; the corresponding standard deviations (STDEV) follow in parentheses.

tures.[15] The average collision cross-sections gradually increased from pentamer to heptamer (Table 1). One charge state of the hexamer (4+) and heptamer (5+) showed two conformers with distinct cross-sections. When the macrocycle size increased further to octamer or decamer, additional conformers were detected. For example, the 5+ ions from octamer **7** were dispersed into at least three conformers with drift times of 1.62, 2.17, and 2.89 ms (Figure S6 in the Supporting Information), leading to collision cross-sections of 695, 873, and 997 Å^2, respectively.

Molecular modeling was employed to gain more information on the precise geometries of the different macrocycles and their cross-sectional areas. For each macrocycle, 150 or 300 structures were energy-minimized by annealing simulations; the resulting collision cross-section versus relative energy plots are shown in Figure 4 and Figures S9–S13 in the Supporting Information. The average collision cross-section of all structures calculated for each macrocycle are included in Table 1, along with the corresponding standard deviations, which are a measure of the range of conformations possible. Note that the counterions were omitted to simplify the modeling,[3d,17] since previous studies revealed that they are highly disordered and difficult to locate accurately in even small self-assembled constructs.[3c,h,10,18] Moreover, fragments generated from a specific charge state by losses of PF_5 maintain almost the same drift time as their parent ions (Figure S6b in the Supporting Information), indicating that the mass of the counterions does not significantly affect the cross-sections of the macrocycles.

Notably, three distinct areas, corresponding to three major families of conformers, can be identified in the plot of collision cross-sections versus relative energies for decamer **8** (Figure 4). Figure 4 includes the average collision cross-section within each area (i.e., for each family of conformers). The computational prediction for the existence of different conformers spanning a wide range of collision cross-sections reconciles the observation of several conformers upon ion-mobility separation. Even though the macrocycles consist of rigid ligands, the flexibility of the whole complex increases with size, leading to a wider range of possible geometries and a higher number of experimentally detected structures for the larger macrocycles. Expectedly, the flexibility is largest for decamer **8**, the size of which permits the formation of substantially different conformers (circular, twisted stretched, twisted folded; Figure 4). For the other macrocycles, the various conformers possible mainly differ in compactness, all having circular shapes (Figures S9–S13 in the Supporting Information).

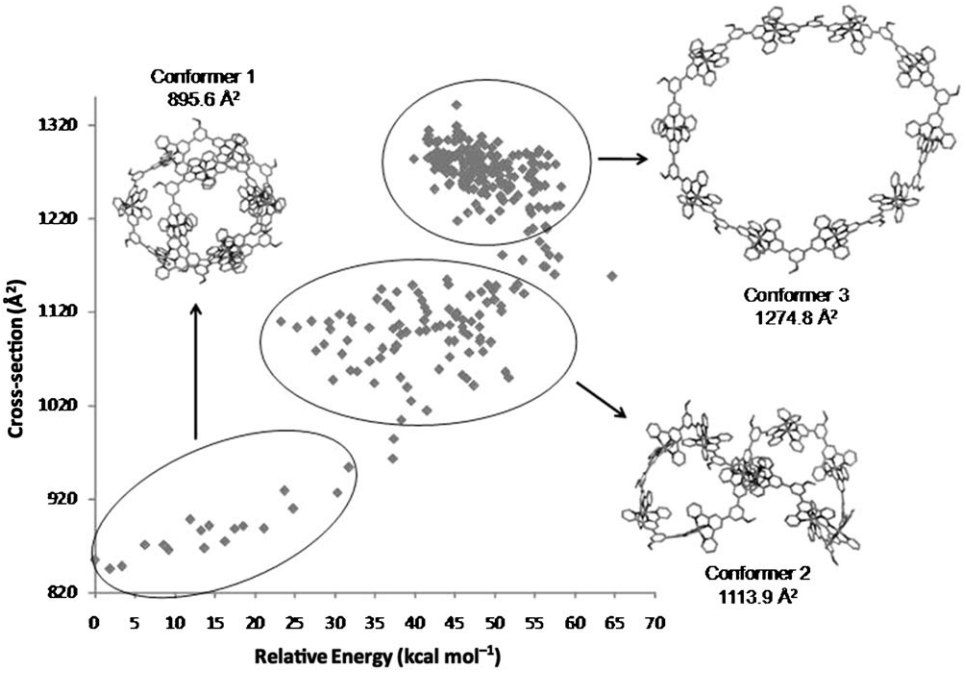

Figure 4. Plot of collision cross-section versus relative energy for 300 structures of complex **8** generated by annealing simulations. The average collision cross-section of all 300 structures is listed in Table 1. The average collision cross-sections of the conformers within the encircled areas are given underneath the corresponding structures.

Also, the ions in low charge states display small collision cross-sections. For instance, 3+ of **3**, 4+ of **4**, 3+ of **6**, 5+ of **7**, and 5+ of **8** gave the smallest collision cross-section compared to the other, higher charge states of the same complex (Table 1). This can be attributed to the lower number of charges resulting in lower charge repulsion and thereby leading to the formation of more compact conformers. The sizes of conformers should thus become larger as the charge states increase, as confirmed by the cross-sectional data of Table 1. In comparison with crystal structures provided by X-ray crystallography and hydrodynamic radii obtained by diffusion-ordered NMR spectroscopy, TWIM-MS captures each conformer and provides size information based on its charge state and drift time. Even though NMR and ESI-MS confirm the composition and connectivity of the different metallocyclic species synthesized, the TWIM-MS technique affords unique and unambiguous insight into the sizes, geometries, and conformational flexibilities of the corresponding cyclic architectures, which would not otherwise be evident.

In summary, a series of homo- and heteronuclear metallomacrocycles with $<$tpy-Fe^{II} (or Ru^{II})-tpy$>$ connectivity has

been successfully synthesized and characterized by means of ^{1}H and ^{13}C NMR spectroscopy as well as ESI mass spectrometry. Larger macrocycles (octamer and decamer) have been achieved by macrocyclization of an extended bis(terpyridine) dimer, thereby eliminating the potential to form smaller cyclic structures. For each self-assembly process, using monomers possessing 120° opposed binding sites, the hexagonal structures always predominate over the other species, which we believe to be derived from the initially formed less stable kinetic products. The combination of TWIM-MS and molecular modeling unambiguously provides size and structure data, as well as monitors the gradual change of flexibility from small to large macrocycles.

Experimental Section

Full experimental details are provided in the Supporting Information.

Acknowledgement

The authors gratefully thank the National Science Foundation (DMR-0812337 and DMR-0705015 to G.R.N.; CHE-1012636 and DMR-0821313 to C.W.) and the Ohio Board of Regents for financial support.

Keywords: conformer separation · macrocycles · mass spectrometry · self-assembly · terpyridine

[1] J.-M. Lehn, *Supramolecular Chemistry: Concepts and Perspectives*, VCH, Weinheim **1995**.

[2] a) B. Hasenknopf, J.-M. Lehn, B. O. Kneisel, G. Baum, D. Fenske, *Angew. Chem.* **1996**, *108*, 1987–1990; *Angew. Chem. Int. Ed. Engl.* **1996**, *35*, 1838–1840; b) B. Hasenknopf, J. M. Lehn, G. Baum, D. Fenske, *Proc. Natl. Acad. Sci. USA* **1996**, *93*, 1397–1400; c) B. Hasenknopf, J.-M. Lehn, N. Boumediene, A. Dupont-Gervais, A. Van Dorsselaer, B. Kneisel, D. Fenske, *J. Am. Chem. Soc.* **1997**, *119*, 10956–10962.

[3] a) M. Schweiger, S. R. Seidel, A. M. Arif, P. J. Stang, *Inorg. Chem.* **2002**, *41*, 2556–2559; b) T. Weilandt, R. W. Troff, H. Saxell, K. Rissanen, C. A. Schalley, *Inorg. Chem.* **2008**, *47*, 7588–7598; c) M. Fujita, O. Sasaki, T. Mitsuhashi, T. Fujita, J. Yazaki, K. Yamaguchi, K. Ogura, *Chem. Commun.* **1996**, 1535–1536; d) S. Hiraoka, M. Fujita, *J. Am. Chem. Soc.* **1999**, *121*, 10239–10240; e) T. Kraus, M. Budesinsky, J. Cvacka, J.-P. Sauvage, *Angew. Chem.* **2006**, *118*, 264–267; *Angew. Chem. Int. Ed.* **2006**, *45*, 258–261; f) O. Mamula, F. J. Monlien, A. Porquet, G. Hopfgartner, A. Merbach, A. von Zelewsky, *Chem. Eur. J.* **2001**, *7*, 533–539; g) F. M. Romero, R. Ziessel, A. Dupont-Gervais, A. Van Dorsselaer, *Chem. Commun.* **1996**, 551–553; h) K. Suzuki, M. Kawano, M. Fujita, *Angew. Chem.* **2007**, *119*, 2877–2880; *Angew. Chem. Int. Ed.* **2007**, *46*, 2819–2822.

[4] N. W. Baxter, J.-M. Lehn, K. Rissanen, *Chem. Commun.* **1997**, 1323–1324.

[5] a) M. Schweiger, S. R. Seidel, A. M. Arif, P. J. Stang, *Angew. Chem.* **2001**, *113*, 3575–3577; *Angew. Chem. Int. Ed.* **2001**, *40*, 3467–3469; b) S. J. Lee, A. Hu, W. Lin, *J. Am. Chem. Soc.* **2002**, *124*, 12948–12949; c) S.-H. Hwang, C. N. Moorefield, F. R. Fronczek, O. Lukoyanova, L. Echegoyen, G. R. Newkome, *Chem. Commun.* **2005**, 713–715; d) T. Megyes, H. Jude, T. Grosz, I. Bako, T. Radnai, G. Tarkanyi, G. Palinkas, P. J. Stang, *J. Am. Chem. Soc.* **2005**, *127*, 10731–10738; e) M. Schmittel, K. Mahata, *Inorg. Chem.* **2009**, *48*, 822–824.

[6] a) M. Fujita, J. Yazaki, K. Ogura, *J. Am. Chem. Soc.* **1990**, *112*, 5645–5647; b) F. A. Cotton, L. M. Daniels, C. Lin, C. A. Murillo, S.-Y. Yu, *J. Chem. Soc. Dalton Trans.* **2001**, 502–504; c) H. Gang, G. Dong, D. Chun-ying, M. Hong, M. Qing-jin, *New J. Chem.* **2002**, *26*, 1371–1377; d) X. Liu, C. L. Stern, C. A. Mirkin, *Organometallics* **2002**, *21*, 1017–1019; e) S.-S. Sun, J. A. Anspach, A. J. Lees, *Inorg. Chem.* **2002**, *41*, 1862–1869; f) S. Ghosh, P. S. Mukherjee, *Inorg. Chem.* **2009**, *48*, 2605–2613.

[7] a) Y.-T. Chan, C. N. Moorefield, M. Soler, G. R. Newkome, *Chem. Eur. J.* **2010**, *16*, 1768–1771; b) S.-H. Hwang, P. Wang, C. N. Moorefield, L. A. Godínez, J. Manriquez, E. Bustos, G. R. Newkome, *Chem. Commun.* **2005**, 4672–4674.

[8] a) P. J. Stang, N. E. Persky, J. Manna, *J. Am. Chem. Soc.* **1997**, *119*, 4777–4778; b) G. R. Newkome, T. J. Cho, C. N. Moorefield, G. R. Baker, M. J. Saunders, R. Cush, P. S. Russo, *Angew. Chem.* **1999**, *111*, 3899–3903; *Angew. Chem. Int. Ed.* **1999**, *38*, 3717–3721; c) G. R. Newkome, T. J. Cho, C. N. Moorefield, R. Cush, P. S. Russo, L. A. Godínez, M. J. Saunders, P. Mohapatra, *Chem. Eur. J.* **2002**, *8*, 2946–2954; d) G. R. Newkome, T. J. Cho, C. N. Moorefield, P. P. Mohapatra, L. A. Godínez, *Chem. Eur. J.* **2004**, *10*, 1493–1500; e) S. R. Halper, S. M. Cohen, *Angew. Chem.* **2004**, *116*, 2439–2442; *Angew. Chem. Int. Ed.* **2004**, *43*, 2385–2388; f) S. R. Halper, S. M. Cohen, *Inorg. Chem.* **2005**, *44*, 4139–4141; g) Y.-T. Chan, X. Li, M. Soler, J. L. Wang, C. Wesdemiotis, G. R. Newkome, *J. Am. Chem. Soc.* **2009**, *131*, 16395–16397.

[9] a) P. L. Jones, K. J. Byrom, J. C. Jeffey, J. A. McCleverty, M. D. Ward, *J. Chem. Soc. Chem. Commun.* **1997**, 1361–1362; b) B. Grossmann, J. Heinze, E. Herdtweck, H. Noth, M. Schwenk, W. Wachter, B. Weber, *Angew. Chem.* **1997**, *109*, 384–386; *Angew. Chem. Int. Ed. Engl.* **1997**, *36*, 387–389; c) H. Jiang, W. Lin, *J. Am. Chem. Soc.* **2003**, *125*, 8084–8085; d) H. Jiang, W. Lin, *J. Am. Chem. Soc.* **2004**, *126*, 7426–7427.

[10] Q. F. Sun, J. Iwasa, D. Ogawa, Y. Ishido, S. Sato, T. Ozeki, Y. Sei, K. Yamaguchi, M. Fujita, *Science* **2010**, *328*, 1144–1147.

[11] J.-L Wang, X. Li, X. Lu, Y.-T. Chan, C. N. Moorefield, C. Wesdemiotis, G. R. Newkome, *Chem. Eur. J.* **2011**, *17*, 4830–4838.

[12] a) M. A. R. Meier, B. G. G. Lohmeijer, U. S. Schubert, *J. Mass Spectrom.* **2003**, *38*, 510–516; b) C. Bazzicalupi, A. Bencini, A. Bianchi, A. Danesi, E. Faggi, C. Giorgi, S. Santarelli, B. Valtancoli, *Coord. Chem. Rev.* **2008**, *252*, 1052–1068; c) U. S. Schubert, H. Hofmeier, G. R. Newkome in *Modern Terpyridine Chemistry*, Wiley-VCH, Weinheim, **2006**, p. 38.

[13] a) X. Li, Y.-T. Chan, G. R. Newkome, C. Wesdemiotis, *Anal. Chem.* **2011**, *83*, 1284–1290; b) S. Perera, X. Li, M. Soler, A. Schultz, C. Wesdemiotis, C. N. Moorefield, G. R. Newkome, *Angew. Chem.* **2010**, *122*, 6689–6694; *Angew. Chem. Int. Ed.* **2010**, *49*, 6539–6544; c) X. Ren, B. Sun, C. C. Tsai, Y. Tu, S. Leng, K. Li, Z. Kang, R. M. V. Horn, X. Li, M. Zhu, C. Wesdemiotis, W. B. Zhang, S. Z. D. Cheng, *J. Phys. Chem. B* **2010**, *114*, 4802–4810.

[14] T. J. Cho, C. N. Moorefield, S.-H. Hwang, P. Wang, L. A. Godínez, E. Bustos, G. R. Newkome, *Eur. J. Org. Chem.* **2006**, 4193–4200.

[15] E. R. Brocker, S. E. Anderson, B. H. Northrop, P. J. Stang, M. T. Bowers, *J. Am. Chem. Soc.* **2010**, *132*, 13486–13494.

[16] a) B. T. Ruotolo, J. L. P. Benesch, A. M. Sandercock, S.-J. Hyung, C. V. Robinson, *Nat. Protoc.* **2008**, *3*, 1139–1152; b) K. Thalassinos, M. Grabenauer, S. E. Slade, G. R. Hilton, M. T. Bowers, J. H. Scrivens, *Anal. Chem.* **2008**, *81*, 248–254.

[17] a) K. Ghosh, J. Hu, H. S. White, P. J. Stang, *J. Am. Chem. Soc.* **2009**, *131*, 6695–6697; b) M. Wang, Y.-R. Zheng, K. Ghosh, P. J. Stang, *J. Am. Chem. Soc.* **2010**, *132*, 6282–6283.

[18] a) N. Takeda, K. Umemoto, K. Yamaguchi, M. Fujita, *Nature* **1999**, *398*, 794–796; b) M. Tominaga, K. Suzuki, M. Kawano, T. Kusukawa, T. Ozeki, S. Sakamoto, K. Yamaguchi, M. Fujita, *Angew. Chem.* **2004**, *116*, 5739–5743; *Angew. Chem. Int. Ed.* **2004**, *43*, 5621–5625.

Received: February 19, 2011
Published online: May 30, 2011

